

Investigating the effect of Shore hardness on the adhesion strength of a gecko robot dry adhesive

Lungile Nyanga^{1,2*}, Reuben Govender¹, Stacey Shield¹, and Abiodun Bayode²

¹Mechanical Engineering, University of Cape Town, Cape Town, South Africa

²Mechanical Engineering, North West University, Potchefstroom, South Africa

Abstract. The hardness of elastomers has been known to be directly related to the Young modulus of elastomers, whereas the Young modulus is generally inversely proportional to the adhesion strength of an adhesive pad. In this research, the Taguchi Design of Experiments was applied to investigate the effect of mixing time, degassing, curing, and post curing temperature on the Shore hardness of Vytaflex 10 pads. The adhesive pressure of the adhesive pads was then measured. The results show that there is an inverse relationship between Shore hardness and adhesive pressure, although the correlation is weak.

1 Introduction

The gecko adhesion mechanism comprises a complex hierarchical system which includes the leg, which facilitates the movement and application of the preload force at a macro scale, the toe, enables the attachment and peeling at a meso scale, nearly half a million setae at a micro scale, and millions of spatulae at a nano scale. The hierarchical structure on the gecko enables adhesion on surfaces with different surface roughness, enables it to attach to uneven surfaces and facilitates the attachment and peeling mechanism [1]. Whereas the gecko adhesion mechanism is based on the spatulae and its hierarchical system for effective adhesion, artificial dry adhesive pads depend on the properties and geometry of the material of the pad [2].

The adhesion force of an adhesive pad is affected by the roughness of the surface on the nanoscale, as presented by the Rabinovich model [3]. The adhesion force is high at very small surface roughness (< 100 nm), decreases to a minimum at a surface roughness of around 200 nm, and then increases again for large surface roughness (> 300 nm) as shown in Fig. 1. This is attributed to the spatula being able to attach well to the surface at a roughness of less than 100 nm, resulting in strong molecular interactions (Fig. 2a). At intermediate roughness between 100 - 200 nm, the spatula can attach to the top of the asperities, resulting in a smaller true contact area and a decrease in adhesion (Fig. 2b). At surface roughness greater than 200 nm, the spatula attaches to the side of the of the asperities which increases the area of contact and adhesion force (Fig. 2c) [3,4]. The adhesive pad attaches to surfaces when a preload force is applied and detach when it is peeled off from the surface. The higher the preload force, the higher the adhesion force if the saturated force is not reached. A greater peeling force is

* Corresponding author: nyangalu@gmail.com

required when a spatula peels at a smaller peeling angle (less than 30°) compared to when the peeling angle is large (greater than 30°) [5,6].

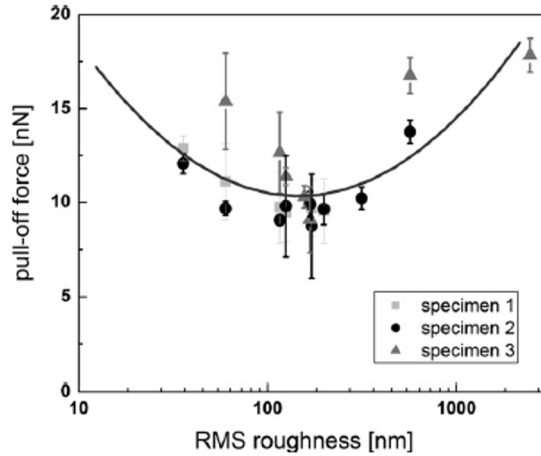


Fig. 1. Relationship between surface roughness and pull-of force [4].

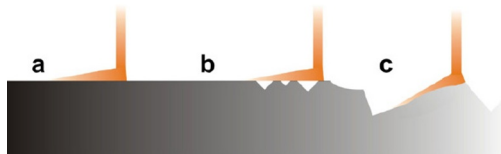


Fig. 2. Spatula adhesion in different surfaces roughness [3].

Adhesion force is generally used when measuring adhesion at nano and micro scale. The measurement used in this paper are at macro scale therefore adhesion strength which is equivalent to the pressure applied by the pad will be used. Practically, the relationship between the Shore hardness and adhesion strength of an adhesive pad is complex. In the literature, no direct relationship between the Shore hardness of a pad and its adhesion strength has been investigated. This is because the effect of other factors such as the adhesion mechanism, surface roughness, shearing motion, stiffness, elastic modulus, pad motion, environmental conditions, and surface energy outweigh the effect of Shore harness on adhesion strength.

The main challenge in trying to investigate a direct relationship between Shore hardness and adhesion strength is that Shore hardness, being a mechanical property of the material, is expected to be constant for all pads made from the same polymer if casted in the same condition. The polymers rarely have Shore hardness sliding across the Shore hardness scale, unless their chemical properties have been altered, which might result in the loss of the desired physical properties, i.e. the adhesion from van der Waals forces in this case. For example, an adhesive pad made from Vytaflex 10 should have a Shore hardness of 10 and is not expected to have a Shore hardness of 20 unless its chemical properties have been altered.

In this research, we investigate how Shore hardness affects the adhesion of a Vytaflex 10 pad to a substrate. The significance of the study is that it will assist in the selection of the material used to fabricate an effective dry adhesive to be used in the development of a wall climbing robot. The expectation is that the lower the Shore hardness of a pad, the higher the adhesion strength as a softer material conforms to a substrate better than a harder one as a softer pad can conform to the profile of the substrate more than a harder pad. Our investigation is twofold; first, we monitor the process parameters during the mixing of the resin and hardener, degassing, during curing, and after curing a Vytaflex 10 pad. The process

parameters investigated are mixing time, degassing method, curing temperature, and post curing temperature. The second part of the investigation is to investigate the effect of Shore hardness on the adhesion strength of a pad.

2 Literature review

2.1 Shore hardness and Young's modulus

A closer correlation between Shore hardness and adhesion strength can be obtained by investigating the relationship between stiffness and Young's modulus with adhesion strength. The adhesion strength of a dry adhesive is affected by the stiffness of its backing layer. At low stiffness during contact, the fibrils can conform to the surface, increasing the adhesion strength. If stiffness increases after initial contact, there is a better load distribution between fibrils, which also increases adhesion strength [7]. The investigations carried out by Gent established that the hardness of an elastomer is directly proportional to Young's modulus, whereas Young's modulus is inversely promotional to the adhesion strength of the pad. This correlation is probably attributed to differences in the strength of the chemical bonds, which affect both the modulus and the tensile strength. A pad with a lower Young's modulus has a higher conformability to the surface, allowing more surface contact and maximising the van der Waals forces acting on the surface [8-10].

2.2 Modification of dry adhesive mechanical properties

The hardness of a polymer can be altered by modifying the chemical or physical structure or the fabrication process [11]. Although the intention might be to alter the hardness of the polymer, it must be noted that other chemical and mechanical properties of the polymer are altered. Chemical modification alters both the chemical and physical properties, while physical modification and process modification mainly alter the physical properties of the polymer.

The mixing time of the urethane resin and hardener determines the initial homogeneity, stoichiometry, and air content of the final product. Inadequate mixing can result in incomplete reactions and under-linked regions, which reduces the joint strength and durability of the urethane [12 - 15]. Vigorous and prolonged mixing leaves air bubbles, lowers the density of the material, and introduces stress concentrators, which degrade the properties of the material.

During moulding, when the elastomer is poured into a mould, air bubbles develop, leading to holes and other defects in a cured dry pad, increasing the porosity of the pad, which affects the Shore hardness of the pad. Degassing the dry adhesive pad can be achieved by vacuum degasification or pressure ovens, which take advantage of Henry's law [16]. The application of a vacuum will create a pressure drop, which reduces the solubility of air in the elastomer, resulting in air bubbles coming out of the elastomer and floating on the surface where they pop, increasing the hardness of the pad. If an elastomer is cured at different vacuum levels, the resultant dry adhesives will have a different hardness.

The cure temperature of the elastomer influences the degree of cross-linking between the elastomer chain molecules, mechanical properties, and adhesion strength [17]. Increasing the post-curing temperature of an elastomer improves its properties by enabling the process of cross-linking of the elastomer molecule chains to be completed, improving the mechanical properties of the dry adhesive [18]. Post-curing also increases the temperature at which molecular mobility begins to take place, resulting in the elastomer transition from the glassy

state to the rubbery state, which improves the adhesive pad's surface hardness, tensile strength, flexural strength, colour stability, and glass transition temperature [19-23].

3 Methodology

In this research, Vytaflex 10 manufactured by Smooth-On was used. The research was carried out on two levels, investigating the process parameters that will produce a Vytaflex10 pad with the smallest Shore hardness and determining the relationship between Shore hardness and adhesion strength. The Taguchi Design of Experiments was applied to determine the effect of mixing time, degassing method, curing temperature, and post-curing temperature on the Shore hardness of the pad. The adhesive pressures of the pads were measured to investigate the relationship between Shore hardness and adhesion strength.

3.1 Taguchi design of experiments

The effect of mixing time, degassing, curing temperature, and post-curing temperature on Shore hardness was investigated at three levels shown in Table 1. The mixing time was the time the Vytaflex resin and hardener are mixed. After mixing, the mixture was slowly poured into 60 *30 mm moulds until the depth is about 10 mm. The moulds were then degassed in a vacuum chamber for 2 minutes and a centrifuge for 5 minutes at the levels and sequence shown in Table 1. Curing was carried out in an air-conditioned room to maintain the temperature for 24 hours. The post-curing was carried out for 8 hours in an air-conditioned room at 25 ° C and in a furnace at 45 ° C and 65 ° C. Eight hours is the recommended time for the heat treatment of Vytaflex according to the manufacturer's recommendation for the post-curing treatment. An air-conditioned environment was used to maintain the temperatures of 20 and 25 ° C. An L9 orthogonal array with a 9-factor level combination was chosen to determine the levels of factors for each experiment. The Shore hardness of the pads was measured according to ISO 7619-2 standard using an Insize Shore A durometer, as shown in Fig. 3(a). For each measurement, the indenter was pressed onto the pad for 5 seconds at each of the positions indicated in Fig. 3(b).

Table 1. Factors and levels of Taguchi experiments.

Factors	Level 1	Level 2	Level 3
Mixing time (min)	2	4	6
Degassing	No degassing (A)	Centrifuge & Vacuum (B)	Vacuum & Centrifuge (C)
Curing Temp (°C)	20	25	30
Post Curing Temp (°C)	25	45	65

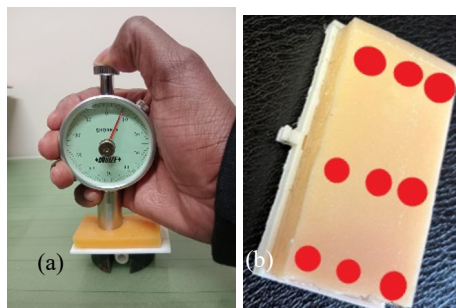


Fig. 3. a) Measurement with durometer. b) Positions of measurement on the adhesive pad.

The Taguchi smaller-the-better signal to noise (S/N) ratio shown in Equation 1 was adopted.

$$\frac{S}{N} = -10 * \log\left(\frac{\sum y^2}{n}\right) \quad (1)$$

where y is the result of each experiment and n is the number of replications of each experiment.

3.2 Adhesion strength measurement method

The adhesion strength of the pad is determined from the force applied to the pad and the area of the pad. The force applied to the pad was measured using the force measurement jig shown in Fig. 4. The force exerted by the pad on the glass was measured by a 5 kg load cell which is calibrated in grams for simplicity as the weights used in the calibration of the load cell are in grams. The real-time data from the load cell were captured using a software called CoolTerm [24]. A plot obtained from CoolTerm showing the preload and adhesion masses (x-axis) against time (y-axis) is shown in Fig. 5.

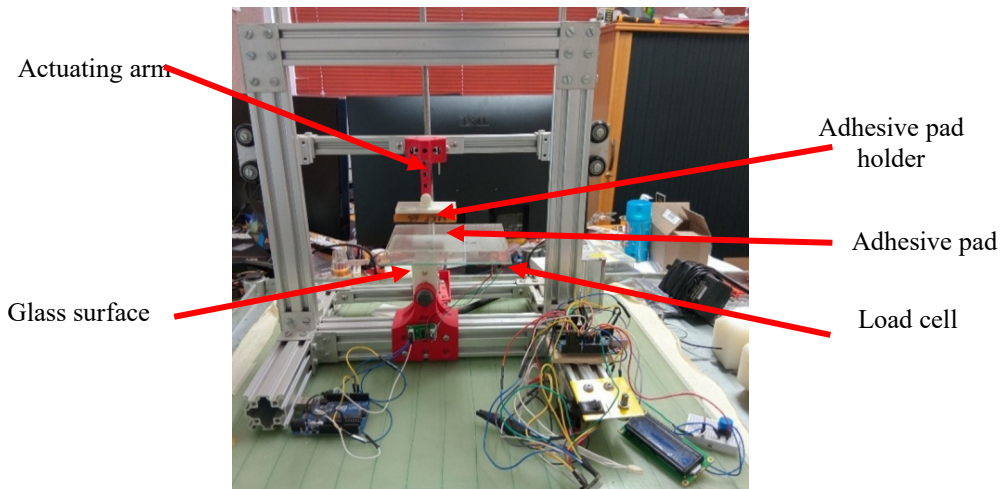


Fig. 4. Force measurement jig.

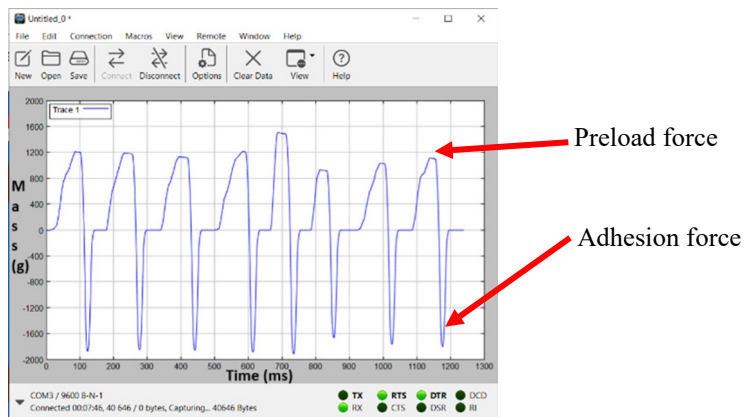


Fig. 5. Preload and adhesion force.

The adhesion strength was assumed to be uniformly distributed and was calculated from the pressure obtained from the jig using the formula.

$$P = \frac{mg}{A} = \frac{(m \cdot 9.81) / 1000}{(0.06 \cdot 0.03)} = 5.4m \text{ Pa} \quad (2)$$

where m is the mass reading from the measuring jig, g is the gravitational acceleration, and A is the cross-sectional area of the dry adhesive in contact with the glass surface.

4 Results and analysis

4.1 Taguchi analysis

The results of the Shore harness obtained from the Taguchi experiments are shown in the L9 orthogonal array in

Table 2. MiniTab [25] was used to determine the responses to the means, S/N ratios, and ANOVA analysis. From the S/N ratios plot in Fig. 6 it can be observed that the best setting to produce an adhesive pad with the lowest hardness is a mixing time of 2 minutes, degassing in a vacuum and then a centrifuge, a curing temperature of 30 °C and a post curing temperature of 65 °C. Shore hardness appears to be more sensitive to the change

Table 2. L9 Orthogonal array.

Trial	Mixing time (min)	Degassing method	Curing temp (°C)	Post-curing temp (°C)	Shore A 1	Shore A 2	Shore A 3	Shore A Average
1	2	A	20	25	10	9,5	10,5	10
2	2	B	25	45	9	9	9	9
3	2	C	30	65	8	8,5	8	8
4	4	A	25	65	9,5	9	9	9
5	4	B	30	25	7,5	7	6,5	7
6	4	C	20	45	10	11	11,5	11
7	6	A	30	45	7	7	6,5	7
8	6	B	25	65	10	10,5	10	10
9	6	C	20	25	9	9	9	9

in curing temperature than other factors. Changes in the mixing time, degassing method, curing temperature, and post-curing temperature appear to have very little effect on the Shore hardness. When considering the ANOVA results shown in Table 3 the factor that affects the hardness the most is the curing temperature followed by the degassing method, then the post-curing temperature and lastly the mixing time. A factor is considered significant if the p-value is less than 0.05 and the F value is very high. All p values except for mixing time are less than 0.05. The curing temperature is the only factor with a very high F value that makes it the only significant factor that corresponds to the results indicated by the S/N values.

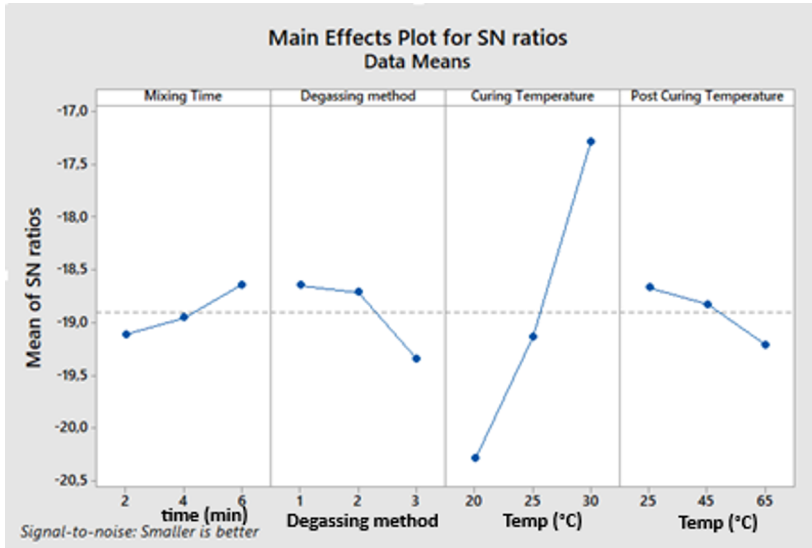


Fig. 6. Main effects plot for SN ratios.

Table 3. ANOVA analysis.

Source	DF	Adj SS	Adj MS	F-Value	P-Value
Mixing Time	2	0,796	0,398	2,53	0,108
Degassing method	2	2,46	1,23	7,82	0,00400
Curing Temperature	2	40,8	20,4	130	0
Post-curing Temperature	2	1,13	0,565	3,59	0,0490
Error	18	2,83	0,157		
Total	26	48,0			

4.2 Relationship between Shore hardness and adhesion strength

The relationship between Shore hardness and the adhesive pad is indicated in Table 4 and Fig. 7. The adhesion strength generally decreases as the Shore hardness increases, although there is a weak correlation between the two, as indicated by the R-Squared value of 0,53 obtained.

Table 4. Shore hardness and adhesion strength.

Shore hardness (A)	Adhesion strength (kPa)
10	4,71
9	4,07
8	5,54
9	4,6
7	4,6
11	3,12
7	5,31
10	3,84
9	4,07

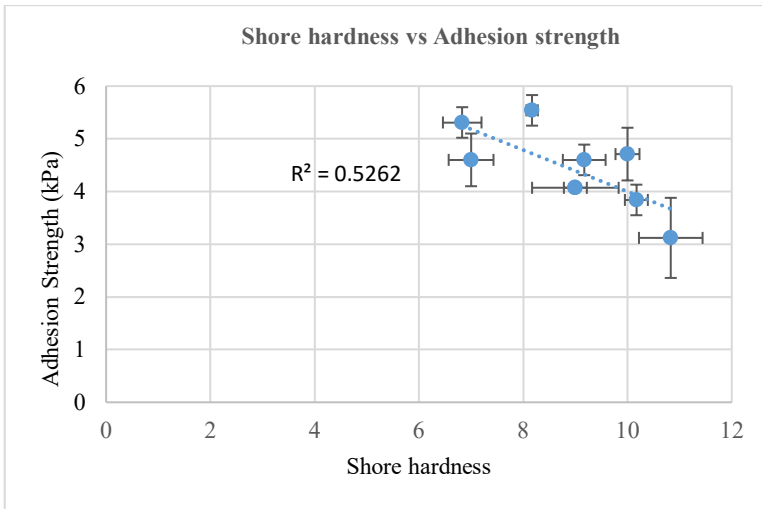


Fig. 7. Relationship between Shore harness and adhesion strength.

5 Discussion

Treating a polymer under different conditions during mixing, degassing, curing, and post-curing can alter the Shore hardness of adhesive pads created by the polymer. Having established that there is a relationship between Shore hardness and adhesion strength, if one wants to continuously improve the adhesion strength obtained from the pads, one will need to determine the optimum curing temperature of the dry adhesive. This is because it is the one that has a significant impact on the Shore hardness of the pad. For further studies, the effect of Shore harness on adhesion strength can be compared with the effect of other physical properties that have been extensively covered in the literature, such as Young's modulus [8-10], stiffness [26], surface roughness [3,4], to determine the physical property that most influences adhesion strength.

The Shore harness measured may also be affected by the heterogeneous material properties resulting from air bubbles remaining in the Vytaflex 10. Further investigation of the distribution of the material characteristics needs to be carried out. This work only focusses on the Shore hardness obtained from Vytaflex 10, which gives a relationship of Shore hardness around 10. The results cannot be extrapolated outside the Shore hardness of 10, since if one wants to obtain Shore hardness of 20, they will need to use a different material, e.g. Vytaflex 20, which has a different chemical composition.

6 Conclusions

The main objective of the research was to determine a direct relationship between Shore hardness and adhesion strength of the Vytaflex 10 elastomer. The Taguchi methods were used to determine the process parameters that will produce an adhesion pad with the least Shore hardness. This was achieved by moulding Vytaflex 10 at different mixing time, degassing, curing, and post curing temperatures levels. The experiments conducted produced adhesive pads with different Shore hardnesses whose adhesion strengths were measured to investigate the relationship between Shore hardness and adhesion strength. The results show that there is an inverse proportional relationship between the Shore hardness and the adhesion strength, although there is a weak correlation.

References

1. W.R. Hansen, K. Autumn, Evidence for self-cleaning in gecko setae, *Proc. Natl. Acad. Sci. U.S.A.* **102**, 385-389, (2005). <https://doi.org/10.1073/pnas.0408304102>
2. Y. Li, J. Krahn, & C. Menon, Bioinspired Dry Adhesive Materials and Their Application in Robotics: A Review. *J Bionic Eng.* **13**, 181–199. (2016). [https://doi.org/10.1016/S1672-6529\(16\)60293-7](https://doi.org/10.1016/S1672-6529(16)60293-7)
3. Y.I. Rabinovich, J.J. Adler, A. Ata, R.K. Singh, and B.M. Moudgil, Adhesion between Nanoscale Rough Surfaces: I. Role of Asperity Geometry, *J Colloid and Interface Science*, **232**, 10–16 (2000)
4. G. Huber, S.N. Gorb, N. Hosoda, R. Spolenak, E. Arzt, Influence of surface roughness on gecko adhesion, *Acta Biomaterialia*, **3**, 607–610, (2007). <https://doi.org/10.1016/j.actbio.2007.01.007>
5. B.N.J. Persson, S.N. Gorb. The effect of surface roughness on the adhesion of elastic plates with application to biological systems. *J Chem Phys*, **119**, 11437–11444, (2003). <https://doi.org/10.1063/1.1621854>
6. K. Autumn, Y.A. Liang, S.T. Hsieh, W. Zesch, W.P. Chan, T.W. Kenny, R. Fearing, & R.J. Full, Adhesive force of a single gecko foot-hair. *Nature*. **40**, 681–685, (2000). <https://doi.org/10.1038/35015073>
7. W. Wang, Y. Liu, & Z. Xie, Gecko-Like Dry Adhesive Surfaces and Their Applications: A Review. *J Bionic Eng* **18**, 1011–1044 (2021). <https://doi.org/10.1007/s42235-021-00088-7>
8. AN. Gent. On the relation between indentation hardness and Young's modulus. *Ruber Chemistry and Technology*, **31**, 896 – 906, (1958). <https://www.doi.org/10.5254/1.3542351>
9. J.Y. Chung, and K.C. Manoj, Soft and hard adhesion, *Journal of adhesion*, **81**, 1119-1145, (2005). <https://doi.org/10.1080/00218460500310887>
10. I.M. Meththananda, S. Parker, M.P. Patel, M. Braden. The relationship between Shore hardness of elastomeric dental materials and Young's modulus. *Dent Mater*, **25**, 956-959, (2009). <https://doi.org/10.1016/j.dental.2009.02.001>
11. W. D. Callister, D. G. Rethwisch, *Materials Science and Engineering: An Introduction*, (John Wiley & Sons, New Jersey, 2018)
12. R. Lomölder, F. Plogmann, F. & P. Speier, Selectivity of isophorone diisocyanate in the urethane reaction influence of temperature, catalysis, and reaction partners. *J. Coatings Technology*, **69**, 51–57 (1997). <https://doi.org/10.1007/BF02696250>
13. C. Brondi, E. Di Maio, L. Bertucelli, V. Parenti, T. Mosciatti, Competing bubble formation mechanisms in rigid polyurethane foaming, *Polymer*, **228**, 123877, (2021). <https://doi.org/10.1016/j.polymer.2021.123877>.
14. Brondi C, Santiago-Calvo M, Di Maio E, Rodríguez-Perez MÁ. Role of Air Bubble Inclusion on Polyurethane Reaction Kinetics. *Materials (Basel)*, **15**, 3132, (2022) <https://www.doi.org/10.3390/ma15093135>
15. M. Hamann, S. Andrieux, M. Schütte, D. Telkemeyer, M. Ranft, W Drenckhan Directing the pore size of rigid polyurethane foam via controlled air entrainment, *J. Cellular Plastics*, **59**, 201-214. (2023) doi:[10.1177/0021955X231152680](https://doi.org/10.1177/0021955X231152680)
16. Y. Zuev. Elastomer–Gas Systems. *International Polymer Science and Technology*, **28**, 43-53, (2001). <https://doi.org/10.1177/0307174X0102800213>

17. L. Léger and C. Creton, Adhesion mechanisms at soft polymer interfaces, *Phil. Trans. R. Soc A*, **366**, 1425–1442, (2008). <https://doi.org/10.1098/rsta.2007.2166>
18. Y. Zhang, R. Adams and L.F.M. Silva, Effects of Curing Cycle and Thermal History on the Glass Transition Temperature of Adhesives. *J of Adhesion*, **90**, (2014). <https://www.doi.org/10.1080/00218464.2013.795116>.
19. J.R. Bausch, C. Delange and C.L. Davidson, The influence of temperature on some physical properties of dental composites. *Journal of Oral Rehabilitation*, **8** 309-317. (1981). <https://doi.org/10.1111/j.1365-2842.1981.tb00505.x>
20. D.A. Covey, S.R. Tahaney, J.M. Davenport, Mechanical properties of heat-treated composite resin restorative materials, *J. Prosthetic Dentistry*, **68**, 458-461, (1992). [https://doi.org/10.1016/0022-3913\(92\)90410-C](https://doi.org/10.1016/0022-3913(92)90410-C)
21. M.A. Loza-Herrero, E. Rueggeberg, W.E. Caughman, G.S. Schuster, C.A. Lefebvre, E. Gardner. Effect of Heating Delay on Conversion and Strength of a Post-cured Resin Composite, *J. Dental Research*, **77**, 426-431, (1998). <https://doi.org/10.1177/00220345980770021201>
22. S.L. Wendt, The effect of heat used as secondary cure upon the physical properties of three composite resins. II. Wear, hardness, and color stability, *Quintessence International*, **18**, 351-356, (1987).
23. G. Cracknell, M. Akay, Kinetics of curing reactions for epoxy-amine / polyethersulphone resins, *J. Therm. Anal*, **40**, 565-573, (1993)
24. R. Meier, CoolTerm, ver 2.4.0, (2025), Available at: <https://freeware.the-meiers.org/>
25. B.F. Ryan, T. A. Ryan and B.L. Joiner, MiniTab, ver 18.1, (2017) Available at: <https://www.minitab.com/en-us/support/downloads/>
26. D. Wang, T. Liu, H. Tian, J. Zhang, Q. He, X. Li, C. Wang, X. Chen, & J. Shao, Stiffness-gradient adhesive structure with mushroom-shaped morphology via electrically activated one-step growth, *Proc. Natl. Acad. Sci. U.S.A.*, **122**, (2025). <https://doi.org/10.1073/pnas.2423039122>